

Multipactor Analysis in Dielectric Resonator Waveguide Filters

R. Keneshloo¹, G. Dadashzadeh², A. Frotanpour³, M. Okhovvat⁴

^{1,2,3}Electrical & Electronic Eng. Dept., Shahed University

⁴Electrical & Electronic Eng. Dept., Imam Hossein University

^{1,2,3} Persian Gulf Highway, Tehran, IRAN, ⁴ babaei Highway, Tehran, IRAN

¹ keneshloo@shahed.ac.ir, ²gdadashzadeh @shahed.ac.ir, ³frotanpour@shahed.ac.ir, ⁴mokhowat@ihu.ac.ir

Corresponding author: G. H. Dadashzadeh

Abstract— Multipactor breakdown analysis is presented in cylindrical dielectric resonator waveguide filter under its dual-mode behavior. The method of effective electron algorithm with combination of Monte-Carlo method is used to perform the simulation and predict multipactor breakdown thresholds. The breakdown thresholds of the proposed structure are presented for different values of frequency-gap product. The results indicate that increasing the radius of filter increases the RF breakdown threshold. The results are compared with the classic parallel plate waveguides.

Index Terms— dielectric resonator, waveguide filters, multipactor breakdown thresholds, effective electron.

I. INTRODUCTION

multipactor is an electron resonance phenomena which occurs in microwave components and transmission lines operating in vacuum [1]. Multipactor electron discharge begins when free electrons within a gap are accelerated by the applied RF field and strike the surface with sufficient energy. Then, secondary electrons release ,follow the same procedure and finally electron avalanche occurs. Electron discharge is dependant upon the space between the surfaces, RF field strength and secondary emission properties of the surfaces. This phenomenon can cause many advers effects in the microwave components such as increasing electric noise, power reflection, detuning of resonant structures, and production of heat [2]. To determine design guidelines, the phenomenon has been analyzed in various types of microwave structures, during recent years,such as parallel plate waveguide[3], rectangular waveguide [4], and coaxial cables[5]. Also, circular and elliptical waveguide has been analyzed under its fundamental mode considering magnetic field [6-7].

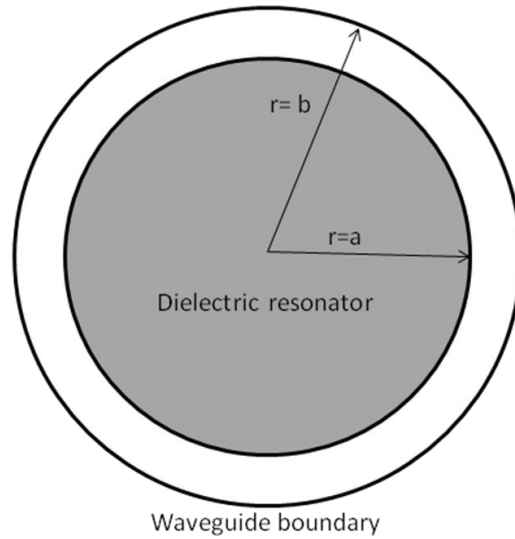


Fig. 1. Cross section of cylindrical dielectric resonator filter

One of the most important microwave component that can be used under high power stage of satellite transponders are dielectric resonator waveguide filters [8]. Dual-mode dielectric resonator filters have been widely used in cellular radios and satellite multiplexers. In satellite multiplexers, improving the spurious performance of such filters will readily translate to higher communication capacity, cost saving, further reduction in weight and size or a combination of these factors [9].

In this paper we present multipactor analysis in dual-mode cylindrical dielectric resonator waveguide filter under the resonant mode of, HE_{11} . First the physical model and mathematical relations including electromagnetic fields, effective electron trajectory and method of multipactor breakdown threshold prediction is presented. Then the simulation is performed and the results of electron trajectory and breakdown thresholds are provided.

II. THEORY AND MODEL DESCRIPTION

The cross section of cylindrical dielectric resonator waveguide filter geometry is shown in Fig. 1. It consists of cylindrical waveguide with radius of $r = b$, which is axially loaded with a concentric dielectric cylinder with radius of $r = a$, and relative permittivity of ϵ_r .

We have considered hybrid mode of HE_{11} for a dual-mode cylindrical dielectric resonator waveguide filter. The electromagnetic fields are as follow [10]:

$$j\omega\mu H_{z_1} = \alpha A J_n(\zeta_1 r) \sin n\phi \quad \text{For } 0 \leq r \leq a \quad (1)$$

$$j\omega\mu H_{z_2} = \alpha A P_n(\zeta_2 r) \sin n\phi \quad \text{For } a \leq r \leq b \quad (2)$$

where A is an arbitrary constant and:

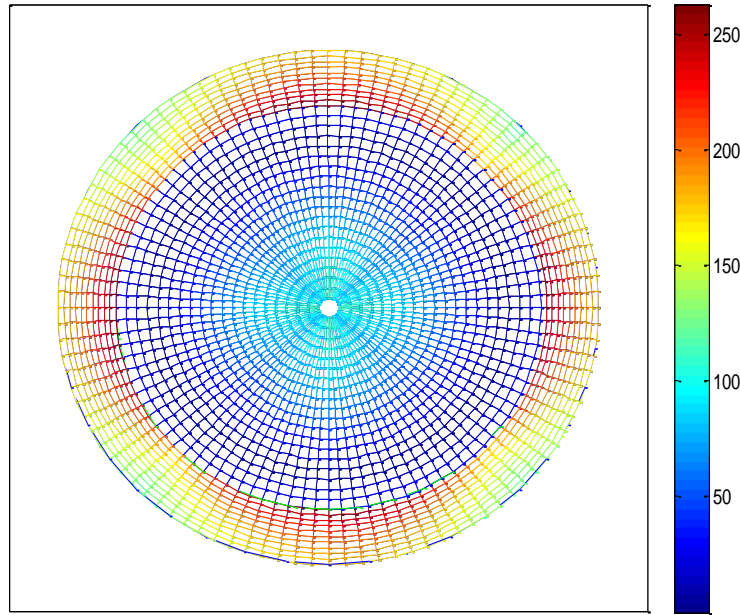


Fig. 2. Field pattern distribution of dual-mode dielectric resonator waveguide filter under HE₁₁ mode.

$$\xi_1^2 = k_1^2 + \gamma^2 ; \quad \zeta_2^2 = -(k_0^2 + \gamma^2) ; \quad \alpha = \frac{-U_n}{aV_n}$$

$$P_n(\zeta_2 r) = J_n(\xi_1 a) \left[\frac{K_n(\zeta_2 r) I_n'(\zeta_2 b) - I_n(\zeta_2 r) K_n'(\zeta_2 b)}{K_n(\zeta_2 a) I_n'(\zeta_2 b) - I_n(\zeta_2 a) K_n'(\zeta_2 b)} \right]$$

$$U_n = n\gamma a J_n(\xi_1 a) \left[\frac{1}{\xi_1^2 a^2} + \frac{1}{\zeta_2^2 a^2} \right] ; \quad V_n = \left[\frac{J_n'(\xi_1 a)}{\xi_1 a} + \frac{P_n'(\zeta_2 a)}{\zeta_2 a} \right]$$

and where $J_n(\cdot)$, $I_n(\cdot)$, and $K_n(\cdot)$ are the Bessel functions, and the modified Bessel functions of the first and second kinds, respectively.

The electromagnetic field distribution of HE₁₁ mode is depicted in Fig. 2. As can be seen the electromagnetic field of a dual-mode dielectric resonator waveguide filter is maximized in horizontal and vertical directions.

To simulate multipactor, we have used the effective electron algorithm in combination with Monte-Carlo method to predict breakdown thresholds [11]. In this method, the effective electron trajectory performs by means of Lorentz electron equation of motion

$$\vec{a} = -\frac{e}{m} (\vec{E}_{total} + \vec{v} \times \vec{B}_{total}) \tag{3}$$

where \vec{v} is the velocity vector; \vec{a} is the acceleration vector; m is the electron mass and e is the electron charge. Also, a DC electric field has been included to properly consider dielectric effect as discussed in [12]. In this case \vec{E}_{total} and \vec{B}_{total} are calculated as follows:

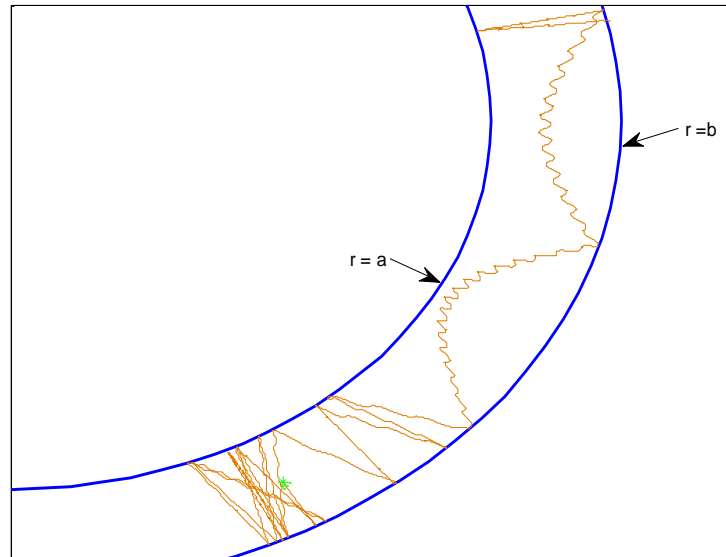


Fig. 3. Electron trajectory for first 30 impacts, $V_e=485\text{v}$, $f=2.49\text{GHz}$

$$\vec{E}_{total} = \vec{E} + \vec{E}_{dc} \quad ; \quad \vec{B}_{total} = \vec{B} \quad (4)$$

where \vec{E} and \vec{B} are the electric and magnetic fields for the proposed structure, respectively. Also, \vec{E}_{dc} is the electric DC field created due to dielectric.

An electron inside the radial gap space between the internal dielectric and the external metallic walls is accelerated by the RF electric field. The movement eventually causes that the electron impacts with waveguide surfaces. Each collision can result in the emission or absorption of secondary electrons. The number of electrons emitted or absorbed after each impact is determined by the value of the Secondary Electron Yield (SEY) parameter. The SEY coefficient based on the impact kinetic energy and incident angle. The trajectory of the electron is tracked by solving its equations of motion by means of the Velocity-Verlet algorithm [6] within the circular dual-mode dielectric resonator waveguide.

The impact velocity and angle is recorded to determine weight of the effective electron. After the impact, a new effective electron is launched from the impact position. The initial velocity and angle of new effective electron is determined using Gaussian distribution and cosine-law distribution, respectively as given in [5].

To predict the multipactor breakdown thresholds, the enhanced counter function is used as described in [11]. This function calculates the weighted sum of the N effective electrons and divides it by the initial total number of effective electrons, N . The weighting of effective

TABLE I. SECONDARY ELECTRON EMISSION PROPERTIES FOR THE MATERIALS

Material	E_{max} (ev)	δ_{max}	E_J (ev)
Silver	165	2.22	30
Copper	250	1.98	25.2
diel _{silver}	165	2.22	30

electrons using the enhanced counter function is performed based on the SEY model of Vaughn's [7] Breakdown threshold is detected if the average of weighting function exceeds from one.

III. SIMULATION RESULTS

The effective electron trajectory has been performed by numerically solving of Eq. 3. A sample of effective electron trajectory is presented in Fig. 3, for 30 numbers of impacts. The dielectric radius, a , is 10mm and the waveguide radius, b , is 12.7mm with the working frequency of 2.49 GHz. ($f \times d = 6.7 \text{GHz} \cdot \text{mm}$). In this figure, the value of the electric field power is 4KW (that is the breakdown threshold for $f \times d = 6.7$). It is equal to $V_e = 485 \text{v}$ (equivalent electric field voltage), calculated by the following equation:

$$V_e = \int_a^b E_r(r, \varphi = 0, \omega t = 0) dr \quad (5)$$

where E_r is the electric field component, a and b are the radius of the cylindrical waveguide and dielectric resonator, respectively.

According to the algorithm described in section II, we have used the enhanced counter function to predict multipactor RF breakdown thresholds. The enhanced counter function uses SEY coefficients for RF breakdown prediction. We have considered 300 effective electrons in the simulation. The number of impact is also obtained to $n=40$ for each effective electron. The results of breakdown converge by employing the proposed values where for more number of impacts and numbers of effective electrons the results remain the same.

The dielectric resonator permittivity is considered to be $\epsilon_r = 37.6$. The parameters of secondary emission yield (SEY) model for dielectric (diel_{silver}), and for waveguide walls (silver, copper) are given in Table I that are extracted from [3]. Diel_{silver} is a fictitious dielectric material, which shares with silver the same SEY properties to have this value for its dielectric permittivity.

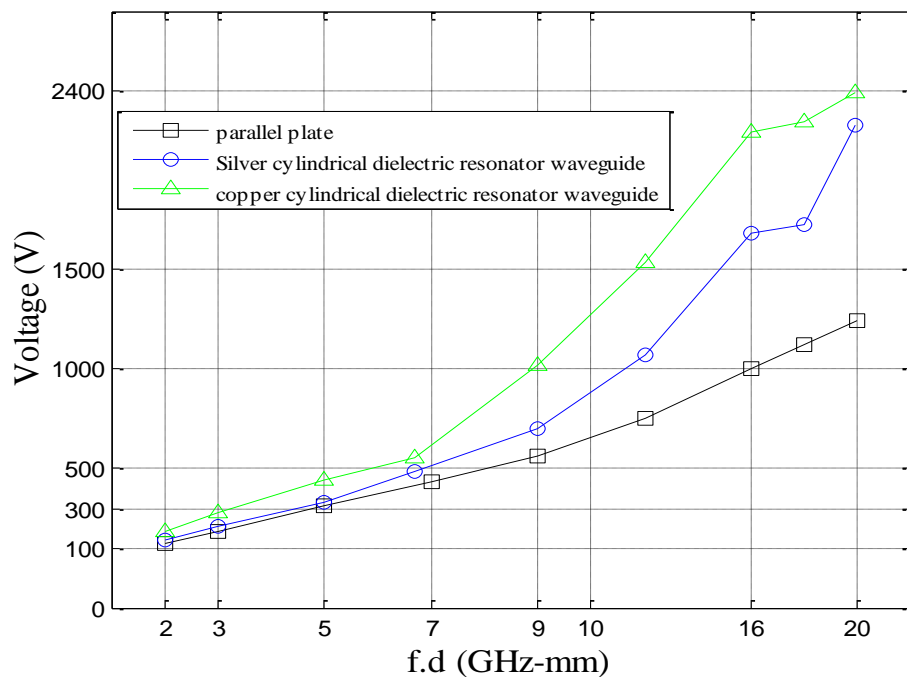


Fig. 4. Multipactor breakdown thresholds for dielectric resonator waveguide filter

The multipactor thresholds have been obtained as a function of the frequency-gap product $f \times d$. The breakdown thresholds are shown in Fig. 4 as function of frequency-gap product for copper and silver material as waveguide wall. These results are also compared with those for the parallel plate waveguide. As can be seen the breakdown threshold increases with increasing $f \times d$ values when these are always above the parallel-plate waveguide thresholds. This means that at the same frequency-gap product $f \times d$, the higher breakdown voltage due to its higher electromagnetic field is obtained for dielectric resonator waveguide filter.

IV. CONCLUSION

The multipactor breakdown has been studied in dielectric resonator waveguide filters. The simulation has been performed under electromagnetic fields of hybrid mode of dual-mode dielectric resonator waveguide filter, HE_{11} . The effective electron approach combined with a Monte Carlo method has been used to predict breakdown thresholds. The RF breakdown voltage threshold has been obtained for these types of filters and it is compared with data for the parallel-plate guide region. Because to their low multipactor breakdown thresholds, using of these filters in the high power stages are critical, and the phenomenon should be considered. The results of the RF breakdown thresholds are always above the parallel-plate waveguide thresholds.

REFERENCES

- [1] J. de Lara, F. Pérez, M. Alfonseca, L. Galán, I. Montero, E. Román, and D. Raboso, "Multipactor prediction for on-board spacecraft RF equipment with the MEST software tool," *IEEE Trans. Plasma Sci.*, vol. 34, no. 2, pp. 476–484, Apr. 2006.
- [2] R. Udiljak, D. Anderson, P. Ingvarsson, U. Jordan, U. Jostell, L. Lapierre, G. Li, M. Lisak, J. Puech, and J. Sombrin, "New method for detection of multipaction," *IEEE Trans. Plasma Sci.*, vol. 31, no. 3, pp. 396–404, Jun. 2003.
- [3] A. Coves, G. Torregrosa-Penalva, C. P. Vicente, A. M. Pérez, B. Gimeno, and V. E. Boria, "Multipactor discharges in parallelplate dielectric-loaded waveguides including space-charge effects," *IEEE Trans. Electron Devices*, vol. 55, no. 9, pp. 2505–2511, Sep. 2008.
- [4] C. Vicente, M. Mattes, D. Wolk, B. Mottet, H. L. Hartnagel, J. R. Mosig, and D. Raboso, "Multipactor breakdown prediction in rectangular waveguide based components," in *Proc. IEEE MTT-S Int. Microw. Symp.*, Long Beach, CA, Jun. 2005, pp. 1055–1058.
- [5] A. M. Pérez, C. Tienda, C. Vicente, S. Anza, J. Gil, B. Gimeno, V. E. Boria, and D. Raboso, "Prediction of Multipactor Breakdown Thresholds in Coaxial Transmission Lines for Traveling, Standing, and Mixed Waves," *IEEE Trans. Plasma Sci.*, vol. 37, no. 10, pp. 2031–2040, Oct. 2009.
- [6] A. M. Perez and V. E. Boria B. Gimeno S. Anza, C. Vicente, and J. Gil, "Multipactor Analysis in Circular Waveguides," *J. of Electromag. Waves Appl.*, vol. 23, no. 11, pp.1575–1583, Sep. 2009.
- [7] A. Frotanpour, G. Dadashzadeh, M. Shahabadi, and B. Gimeno, "Analysis of multipactor RF breakdown thresholds in elliptical waveguides," *IEEE Trans. Electron Devices*, Dec. 2010.
- [8] R. J. Cameron, C. M. Kudsia, and R. R. Mansour "Microwave filters for communication systems: fundamentals, design, and applications", Wiley-Interscience, 2007.
- [9] Ian Hunter, "Theory And Design Of Microwave Filters", The Institution of Electrical Engineers, London, United Kingdom,2001.
- [10] K. A. Zaki and A. E. Atia, 'Modes in dielectric-loaded waveguides and resonators,' *IEEE Trans. Microw. Theory Tech.*, vol. MTT- 31, pp. 1039-1045, Dec. 1983.
- [11] E. Somersalo, P. Ylä-Oijala, D. Proch, and J. Sarvas, "Computational methods for analyzing electron multipacting in RF structures," *Part. Accel.*, vol. 59, pp. 107–141, 1998.
- [12] G. Torregrosa, Á. Coves, C. P. Vicente, A. M. Pérez, B. Gimeno, V. E. Boria, "Time Evolution of an Electron Discharge in a Parallel-Plate Dielectric-Loaded Waveguide" *IEEE Electron Device Lett.*, vol. 27, no. 7, pp. 619–621, Jul. 2006.